Stochastic Modeling of Cooperative Multi-Hop Networks with Lognormal-Rice Fading

By

Muhammad Bilal Haroon

NUST201260865MSEECS61212F

Supervisor

Dr. Syed Ali Hassan

Department of Electrical Engineering

A thesis submitted in partial fulfillment of the requirements for the degree of Masters in Electrical Engineering (MS EE-TCN)

In

School of Electrical Engineering and Computer Science,

National University of Sciences and Technology (NUST),

Islamabad, Pakistan.

(August 2015)

Approval

It is certified that the contents and form of the thesis entitled "**Stochastic Modeling of Cooperative Multi-Hop Networks with Lognormal-Rice Fading**" submitted by **Muhammad Bilal Haroon** have been found satisfactory for the requirement of the degree.

Advisor: **Dr. Syed Ali Hassan**

Signature: _____

Date: _____

Committee Member 1: **Dr. Khawar Khrshid**

Signature: _____

Date: _____

Committee Member 2: **Dr. Adnan Khalid Kiani**

Signature: _____

Date: _____

Committee Member 3: **Dr. Ali Haider**

Signature: _____

Date: _____

Dedication

I dedicate this thesis to my parents, my sister, my brother and teachers who helped me throughout my research phase.

Certificate of Originality

I hereby declare that this submission is my own work and to the best of my knowledge it contains no materials previously published or written by another person, nor material which to a substantial extent has been accepted for the award of any degree or diploma at National University of Sciences & Technology (NUST) School of Electrical Engineering & Computer Science (SEECS) or at any other educational institute, except where due acknowledgement has been made in the thesis. Any contribution made to the research by others, with whom I have worked at NUST SEECS or elsewhere, is explicitly acknowledged in the thesis.

I also declare that the intellectual content of this thesis is the product of my own work, except for the assistance from others in the project's design and conception or in style, presentation and linguistics which has been acknowledged.

Author Name: **Muhammad Bilal Haroon**

Signature: _____

Acknowledgment

I am very thankful to Allah who gave me strength, support and bestowed HIS special blessing on me, without all of this it cannot be possible for me to complete my research.

I am eternally grateful to my family who have always supported me by their encouragement and by moral and emotional support throughout the dissertation. This thesis is a milestone in my academic carrier. Extensive research has increased my knowledge in learning theories and concepts.

I express my deepest gratitude to Dr. Syed Ali Hassan, my advisor and my mentor, who provided me with his esteemed assistance and valuable thoughts in my whole research work. His recommendations and advices have enabled me to fulfill the requirements of the thesis work and allowed me to follow the path of success in this research.

I would like to thank my honourable committee members, Dr. Khawar Khurshid, Dr. Adnan Khalid Kiani, Dr. Ali Haider and to all those teachers who contributed towards the successful completion of my dissertation. At last but not the least my special thanks to all my friends and colleagues who were always there for me.

Muhammad Bilal Haroon

Abstract

In this thesis, we present an analytical model for a cooperative multi-hop network subject to a deterministic and random path loss wireless channel. For deterministic case, we present the model for a multi-hop two- dimensional (2-D) network with finite density of nodes communicating with one another by forming an opportunistic large array. The wireless channel is considered as a composite lognormal-Rice random process. We approximate the sum distribution of the received power at a node with lognormal random variable (RV) using a moment generating function (MGF)-based approach, which is acquired by using Gauss-Hermite integration. In random path loss model, a strip-shaped sensor network is considered, where randomly placed nodes communicate cooperatively. The distribution of received power at a node is calculated as a three step process, which includes finding the distribution of random distance between nodes in addition to other channel impairments, i.e., fading and shadowing. It is shown that in the presence of all three channel impairments, the received power at a node follows a lognormal distribution. The system performance and coverage range of the network are quantified as a function of various network parameters and node topologies. The theoretical results are validated by performing computer simulations.

Table of Contents

List of Figures

Chapter 1

Introduction

Ever growing increase for efficient and reliable data delivery in future wireless systems suggests the use of cooperative transmission (CT). CT suppresses the issues of high latency and low reliability by employing distributed single-antenna nodes that receive multiple copies of the same message signal, thereby providing spatial diversity. The spatial diversity improves the received signal-to-noise ratio (SNR) by limiting the effects of multipath fading and shadowing present in a wireless channel. Dense wireless sensor network (WSN), following a multi-hop arrangement, widely uses CT for communication. The deployment of sensor networks can be used where low-power and low-cost data accumulation is required, such as, monitoring and controlling indoor temperature [1] or broadcasting of abnormal traffic events [2].

Opportunistic Large Arrays (OLAs), [3], is one of the most effective CT techniques used at the physical layer, where the nodes in a multi-hop network form groups, and these groups communicate with each other cooperatively. Transmission takes place in pre-synchronized time slots because each group is assumed to have prior preamble synchronization for symbol and time co-

ordination and easy channel access [4]. All nodes in a group receive the same message signal and the receiving nodes try to decode the message using a diversity scheme and become part of the transmitting nodes towards next group. In densely populated networks, OLA provides a promising feature of long distance broadcasting with less power consumption.

Cooperative transmission, as a physical layer transmission technique, was introduced to boost the system efficiency by employing spatial diversity. The system capacity increases by providing distributed transmit diversity as multiple nodes transmit the same message and in lieu of that a node receives multiple copies of the same message, which increases the likelihood of decoding the message correctly. OLA that perform in a multi-hop manner where all nodes in a network form groups, and these groups of nodes transmit the same message at the same time to the other group. The promising feature of range extension [10, 11] due to OLA broadcasting and energy efficiency [21] makes it a desirable option for densely populated networks.

In a wireless channel, the radio propagation under-goes sufficient amount of distortion and attenuation from its surroundings. In literature, various studies were made to analyse the effects of multipath fading in cooperative networks, most of them had considered Rayleigh fading as the only channel impairment along with path loss. However, in a wireless system the effect on signal propagation in the presence of lognormal shadowing is significant, which is another important step while moving towards the practical scenarios. In addition to shadowing, if we move to the more realistic scenario of deploying a chain of nodes communicating cooperatively, we can see that the possibility of having a line-of-sight (LOS) component increases specially in

outdoor environment. Even in indoor, we can have a LOS component. This LOS causes a great shift in mean estimations for decoding signal correctly. To our knowledge, no research is been conducted to consider the composite Rician fading and lognormal shadowing for analysing the performance of OLA networks.

1.1 Problem Statement

Previous work only cater the Rayleigh fading enviornment along with path loss while modeling the cooperative communication in WSN. This gap arises the question of what will be the effect of anomalies created by LOS signal? How the presence of large buildings in the vicinity of sensor deployment going to effect the system? what will be the effect of random path loss?. Considering the unanswered questions we made our problem statement as

"To determine the coverage range for the OLA network by enabling cooperation between nodes, while incorporating Rice fading, path loss, and lognormal shadowing effected channels as independent channel impairment parameters for stochastic geometries of nodes "

1.2 Thesis Contribution

The objective of this thesis is to analyze how cooperative communication helps the sensor nodes in the presence of composite fading. For that we derive the analytical expression for two separate models differentiated interms of deterministic and random path loss. For each model we derived the signal-to-noise ratio (SNR). We then further derive the one-hop success

probability for both the networks. Our contributions include the derivation of the probability density function (PDF) of SNR at a node, which is a stochastic process that includes a ratio distribution of a lognormal random variable (RV) and random distance RV, along with Rice fading. The effect on network's coverage area is quantified as a function of path loss exponent, Rice K-factor and standard deviation of shadowing. We have shown that an increase in the severity of shadowing badly impacts the performance of network, whereas, incorporating the LOS component increase the coverage range of the network under consideration.

1.3 Thesis Organization

The rest of the thesis is organized as follows: Chapter 2 describes the related work that are done in the domain of OLA networks. Chapter 3, we present the system model for a two-dimensional (2-D) extended networks subject to composite lognormal-Rice fading along with the deterministic path loss. In chapter 4, we propose a geometric model for a 2-dimensional (2D) strip-shaped OLA network where each node broadcasts the message by using decode-and-forward (DF) technique, whereas, the wireless channel undergoes lognormal shadowing and Rice fading along with random path loss. Chapter 4 also include the derivation of the probability density function (PDF) of SNR at a node, which is a stochastic process that includes a ratio distribution of a lognormal random variable (RV) and random distance RV, along with Rice fading. Some numerical results for various sets of parameters follow in chapter 5. In chapter 6, conclusion and future work is discussed.

Chapter 2

Literature Review

Data gathering, possibly in a multi-hop fashion, from a wide spread of unknown amount of sensors to a sink node is an important application of WSN. Each sensor node in the path of a transmission is responsible for relaying the message to another node. However, issues of long delays, low reliability, and increased latency raised serious questions on the performance of single-input single-output (SISO) multi-hop networks. In addition to that, the channel impairments like multipath fading and shadowing limit the performance of the system.

Opportunistic large arrays (OLAs) [5] is one of the most effective CT techniques used at the physical layer, where the nodes in a multi-hop network form groups, and these groups communicate with each other cooperatively, [5]. Transmission takes place in pre-synchronized time slots because each group is assumed to have prior preamble synchronization for symbol and time coordination and easy channel access [4, 6]. All nodes in a group receive the same message signal and the receiving nodes decode the message using a diversity scheme and become part of the transmitting nodes towards next

group. In densely populated networks, OLA provides a promising feature of long distance broadcasting with less power consumption [10].

A considerable amount of research is done in practical implementation of CT such as, [7]-[9]. Similarly, numerous authors have exploited the various properties of OLA. In [19], Mergen *et al* used *continuum* approximation approach, i.e., fixed amount of transmit power per unit area along with infinite density of nodes. Although their model ensures end-to-end delivery but the study provided asymptotic results for very large density of nodes. On the other hand, there is generally a finite node density in wireless networks and infinite propagations are prohibited. For finite number of nodes, a linear network model is proposed in [20]. The analytical model depicts the successful finite number of hop counts before the transmission fails for a fixed distance between nodes. A 2-dimensional strip network is considered in [21], where authors studied the energy efficiency of an OLA strip network. Transmission protocols involving OLA, such as OLAROAD [22] and OLACRA [23] define cooperative route spans constructed over strip-shaped multi-hop networks.

The radio propagation under-goes sufficient amount of distortion and attenuation from its surroundings. In literature, various studies were made to analyse the effects of multipath fading in cooperative networks, most of them had considered Rayleigh fading as the only channel impairment along with path loss [13, 14, 15]. However, in a wireless system the effect on signal propagation in the presence of lognormal shadowing is significant, which is another important step while moving towards the practical scenarios. A line network with composite Rayleigh fading and independent shadowing was studied in [16], whereas the effect of correlated shadowing are quantified in

[17] for the same 1-dimensional network. In addition to shadowing, if we move to the more realistic scenario of deploying a chain of nodes communicating cooperatively, we can see that the possibility of having a line-of-sight (LOS) component increases specially in outdoor environment. Even in indoor, we can have a LOS component as shown in [18]. This LOS causes a great shift in mean estimations for decoding signal correctly. To our knowledge, no research is been conducted to consider the composite Rician fading and lognormal shadowing for analysing the performance of OLA networks.

In addition to this, the arbitrary positioning of nodes has short term effects on the network performance but their characteristics can be more drastic. In literature, a considerable amount of studies can be found on OLA networks under the impact of multipath fading, however, only Rayleigh fading model is widely used along with path loss [24]-[28]. This assumption may be used for simple network analysis, however, to gain practical insights into the network coverage, all major factors that impair wireless propagation should be considered. Generally, we characterize the fading phenomenon to be small-scale or large-scale.

Chapter 3

Lognormal-Rice Fading with Deterministic Path loss

In this chapter, we consider the model for a two-dimensional (2-D) extended networks under composite lognormal-Rice fading, whereby, a group of nodes cooperatively transmit the same message to another group of nodes and model the transmission from one group to another as a discrete-time Markov chain. The received signal, at a particular node, is a sum of multiple transmitted signals over orthogonal channels [30]; each of this signal experiences small-scale fading as well as shadowing. To find the success probability of a node, the required probability density function (PDF) for the sum of composite lognormal-Rice random variables (RVs) is computed using Guass-Hermite numerical computation, which is composed by using a moment generating function (MGF)-based approach [31]. By using Gauss-Hermite integration, the MGF of the sum distribution is approximated to a single log-normal RV, where we use its mean and variance to determine the effect on network's coverage area. The effect on network's coverage area is quantified as a function

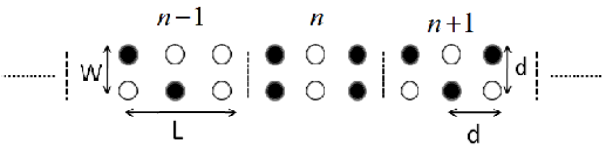

Figure 3.1: A 2D grid network with $L = 3, W = 2; M = 6$

of path loss exponent, Rice K-factor and standard deviation of shadowing.

3.1 Network Model

We consider an extended network in the form of a horizontal strip, with finite number of nodes, placed in a two-dimensional formation as shown in Fig. 3.1. Each node is placed at a distance d from its neighbouring nodes in both dimensions. Let L denotes the number of nodes per hop along the horizontal stretch and W be the width of the network, representing the number of nodes in the vertical dimension, as shown in Fig. 3.1. Correspondingly, we define $M \triangleq L \times W$ to be the number of nodes in one level forming an OLA that cooperates synchronously to transmit the same message to next level (or OLA) containing other M number of nodes. The cooperative mechanism of decode-and-forward (DF) is used.

The message will propagate from hop to hop, when a node, in any level, receives a message and at least one node from the previous level transmits. However, error-free decoding of the message depends upon the received signal-to-noise ratio (SNR) being greater than or equal to a certain threshold, τ. In Fig. 3.1, a node that satisfies the threshold criterion and becomes a DF node is filled with black, while the hollow circles show the nodes that

failed to decode the message. The different levels are represented as n-1, n, n+1 etc. Our assumptions include that all the nodes have same transmit power, P_t; each transmission is done over orthogonal fading channel, and all receivers have perfect timing and frequency synchronization.

To represent the nodes in a system, let us define some notations, which would be used throughout this paper. The nodes in the network are labeled from top to bottom and left to right, in a level. At a level n, the indices of the nodes that decoded the message without any error are represented by a set $\mathbb{N}_n$. For example, $\mathbb{N}_n = \{1, 2, 5, 6\}$ and $\mathbb{N}_{n+1} = \{1, 4, 5\}$, for the case of Fig. 3.1. If a node m at level n is transmitting to a node j at level $n + 1$, then the received power, P_r , at the j^{th} node is given as

$$P_{r_j}(n+1) = \frac{P_t}{d^\beta} \sum_{m \in \mathbb{N}_n} \frac{\nu_{mj}}{\left(\sqrt{\delta_{mj}}\right)^\beta}. \tag{3.1}$$

In the above equation ν_{mj} is a composite fading coefficient that represents the small-scale as well as large-scale channel fading between node j in the current level and node m in the previous level. The large-scale shadowing is modeled as log-normal random process, whereas Rice fading is used to model the effects of small-scale fading. The Path loss exponent, represented as β, ranging between 2-4. The distance between nodes m and j is given by a Euclidean metric $\sqrt{\delta_{mj}}$.

3.2 Modeling By Markov chain

In this section, we develop a one-hop transmission model, keeping in view that a node at level n can only participate if at least one node in level

$n-1$ has transmitted and that node also decodes the message correctly. At a particular time instant, all nodes in a level can decode the data or not, therefore, we can represent the nodes as in 'on' or 'off' state, either '1' or '0', respectively. As mentioned earlier the nodes are labeled from top to bottom and left to right, the state of a node in a certain level n can be given as

$$\tilde{\mathcal{X}}(n) = \begin{bmatrix} \mathbb{I}_{1,1}(n) & \mathbb{I}_{2,1}(n) & \cdots & \mathbb{I}_{L,1}(n) \\ \mathbb{I}_{1,2}(n) & \vdots & \ddots & \vdots \\ \vdots & \vdots & \ddots & \vdots \\ \mathbb{I}_{1,W}(n) & \mathbb{I}_{2,W}(n) & \vdots & \mathbb{I}_{L,W}(n) \end{bmatrix} \tag{3.2}$$

where $\mathbb{I}_{i,j}(n)$ is the binary indicator random variable representing the state of a node in i^{th} position horizontally and j^{th} position vertically, where $i = \{1, 2, \ldots, L\}$ and $j = \{1, 2, \ldots, W\}$. The subscript act as a coordinates for row and column in which the node is present. From Fig. 3.1 $\mathbb{I}_{1,1}(n) = 1, \mathbb{I}_{1,2}(n) = 1, \mathbb{I}_{2,1}(n) = 0$; $\tilde{\mathcal{X}}(n) = \begin{bmatrix} 1 & 0 & 1 \\ 1 & 0 & 1 \end{bmatrix}$. We can now convert our 2-D model into 1-D by defining $\mathcal{X}(n) = \{vec[\tilde{\mathcal{X}}(n)]\}^T$, here a vector operation, *vec*, is performed to convert the 2-D matrix in to single dimension column vector and T denotes the transpose operator. For instance, from Fig. 3.1, $\mathcal{X}(n) = [110011]$.

This tends to confer an M-bit binary outcome for each hop, forming a state, and there are 2^M possible states. Since at a certain time instant n, the current state node only depends upon the previous state, hence $\mathcal{X}(n)$ can be regarded as a discrete-time Markov Process. The discrete-time assumption comes from the fact that the transmissions occur at every distinct slots synchronously [33]. Markov chain with state space, $\mathbf{S}$, given M number of

nodes per state, can be represented as $\mathbf{S} = \{0, 1, 2, \ldots, 2^M - 1\}$. Here we assume that the channel between levels exhibits the same statistics (in terms of channel fading) and each node have the same transmit power; hence the Markov chain is regarded as homogeneous.

Furthermore, there is a probability that at some point, none of the nodes in a level is able to decode the message correctly, implying that the Markov chain is in state $\{0\}$ resulting in no further transmission, $\lim_{n\to\infty} \mathbb{P}\{\mathcal{X}(n) = 0\} \nearrow 1$.. We are now in a position to define the state transition matrix for our Markov chain. Our state space is defined as $\mathbf{S} = \{0\} \cup \mathbf{A}$, where $\mathbf{A} = \{1, 2, ...2^M - 1\}$ is irreducible transient space set and 0 is absorbing state. If we define $\hat{\mathbf{P}}$ as transition probability matrix with state space $\mathbf{S}$ then by removing the first column and row that involves transitions to and from absorbing state, we are left with matrix $\mathbf{P}$, which is a sub-matrix of $\hat{\mathbf{P}}$ comprising of states $\mathbf{A} \subseteq \mathbf{S}$ with dimension $(2^M - 1) \times (2^M - 1)$.

Since $\mathbf{P}$ is a square irreducible and non-negative matrix, then by Perron-Frobenius theorem [34], a unique maximum eigenvalue, ρ, exists with a unique eigenvector associated with it. As $\mathbf{P}$ is not truly right stochastic due to eliminating of absorbing state, the Perron eigenvalue is always less than one, i.e., $\rho < 1$. If $\mathbf{u}$ is the left eigenvector of transition matrix $\mathbf{P}$, then $\mathbf{u} = (u_i, i \in A)$ is called ρ-invariant distribution and it describes the state of the system before going into absorbing or killing state and is called quasi-stationary distribution. At time n, probability of being in a state j is

$$\mathbb{P}_r\{\mathcal{X}(n) = j\} = \rho^n u_j, j \in \mathbf{A}, n \geq 0 \quad . \tag{3.3}$$

If we define $\mathcal{K} = inf\{n \geq 0 : \mathcal{X}(n) = 0\}$ as end of transition time then probability, until killing occurs is, $\mathbb{P}_r\{\mathcal{K} > n + h | \mathcal{K} > n\} = \rho^h \quad$. Hence

quasi-stationary distribution for the Markov chain becomes

$$\mathbb{P}\{\mathcal{X}(n) = j|\mathcal{K} > n\} = u_j, j \in \mathbf{A}, \quad \forall n \quad . \tag{3.4}$$

3.3 Formulation of the Transition Matrix for Deterministic Path loss Network

In this section, we find the transition probability matrix, $\mathbf{P}$, for our model, the eigenvector of which will give us the quasi-stationary distribution. Let us define the source and destination states as i and j, respectively. Note that i and j are the decimal equivalent representations of the pair of states of the system, such that $i, j \in \mathbf{A}$. For instance, for $M = 6$, as show in Fig. 1, if transition is going from $\{100100\}$ to $\{110011\}$ then $i = 36$ and $j = 51$.

At a particular node, we receive signals from various paths, each of which undergoes shadowing and multipath fading; the number of paths depends upon the number of transmitting nodes (number of 1's) in the previous level (state). The received SNR at the kth node of level n can be given by $\gamma_k(n) = P_{rk}(n)/\sigma_N^2$, where, σ_N^2 is variance of white noise, which is assumed equal for all nodes in a level, and P_r is the received power as given in (3.1). The conditional probability for the receiving node k to successfully decode the message at time n is given as

$$\begin{aligned} \mathbb{P}_r\{\text{Success of node k}|\varepsilon\} = \mathbb{P}_r\{\mathbb{I}_k(n) = 1|\varepsilon\} = \\ \mathbb{P}_r\{\gamma_k(n) > \tau|\varepsilon\} = \int_\tau^\infty p_{\gamma k|\varepsilon}(z)\,\mathrm{d}z \quad , \end{aligned} \tag{3.5}$$

Here the event, $\varepsilon \in \mathcal{X}(n-1)$, indicates that previous state is transition state and, $p_{\gamma k|\varepsilon}(z)$ is the conditional probability density function (PDF) of

the received SNR. Similarly, the probability for the receiving node being in outage is given by $1 - \mathbb{P}_r\{\gamma_k(n) > \tau|\varepsilon\}$. It can be noticed that the received SNR is a sum of lognormal-Rice RVs, for which the distribution for sum of lognormal-Rice RVs does not exists in closed-form [35]. Therefore, a moment generating function (MGF) technique is used to find the sum of lognormal-Rice RV. In this method, the sum of independent RVs can be expressed as the product of the MGFs of individual RVs.

We first define a composite RV, $\nu = W\phi$; where W is a Rician RV and ϕ is a lognormal RV. Then we approximate the sum of K lognormal-Rice RVs $(\nu_1, \nu_2, \ldots, \nu_K)$ by a single lognormal RV. One way to model this is to equate the PDF of the resultant lognormal RV, ϕ, with the convolutions of the PDFs of individual ν_i's; however, a closed-form expression is prohibited. Another method is to equate the MGF of ϕ with the product of MGFs of ν_i and then find the mean and variance of ϕ in terms of the parameter of individual ν_i's. We use the latter approach. Now for the sum of K lognormal-Rice RVs, $\sum_{k=1}^{K} \nu_k = (\nu_1, \nu_2, \ldots, \nu_K)$, the MGF is given as

$$\Psi_{\phi}(\nu_1, \nu_2, \ldots, \nu_K) = \prod_{k=1}^{K} \Psi_{\nu_k}(s; \mu_k, \sigma_k, \kappa_k) \quad . \tag{3.6}$$

Where μ_k and σ_k are the mean and standard deviation of the kth lognormal RV and κ_k, is the Rice factor for the k^{th} Rician RV. This approximation method requires a closed-form expression for the MGFs of both the lognormal-Rice and lognormal RVs. However, it is difficult to find them in a closed-form so for that we used a Gauss-Hermite integration, which provides an easy solution of their numerical computation. The MGF approximation

of the lognormal RV ϕ_k, by using the Gauss-Hermite integration is given as

$$\widehat{\Psi}_{\phi}(s;\mu_X,\sigma_X) = \sum_{n=1}^{N} \frac{w_n}{\sqrt{\pi}} \exp\left[-s \exp\left(\frac{\sqrt{2}\sigma_X a_n + \mu_X}{\xi} \right) \right]. \tag{3.7}$$

Where μ_X and σ_X are the mean and standard deviation of the Gaussian RV $X = 10\log_{10}\phi$. In Gauss-Hermite integration, the integral is estimated by an approximate sum where the summation is defined by specific weights. The MGF of k^{th} lognormal-Rice RV by Gauss-Hermite integration can be written as

$$\begin{aligned} \widehat{\Psi}_{\nu_k}(s;\mu_k,\sigma_k,\kappa_k) = \sum_{n=1}^{N} & \frac{{}^{w_n(1+\kappa_k)}/_{\sqrt{\pi}}}{1+\kappa_k + s\exp(\frac{\sqrt{2}\sigma_k a_n + \mu_k}{\xi})} \\ & \times \exp\left(- \frac{s\kappa_k \exp(\frac{\sqrt{2}\sigma_k a_n + \mu_k}{\xi})}{1+\kappa_k + s\exp(\frac{\sqrt{2}\sigma_k a_n + \mu_k}{\xi})} \right) \quad . \end{aligned} \tag{3.8}$$

The Hermite integration order, N, is used to achieve better estimate of mean and standard deviation the larger the value of N the better the estimate. The adjustable parameter s of the MGF with positive real values gives two independent equations from which μ_k, and σ_k^2 are calculated. Where $\xi = 10/\ln 10$, is a constant for scaling and w_n is the weight corresponding to the abscissas, a_n. In [36] the values for N along with the corresponding weights and abscissas can be found in a tabulated form. By finding individually for each RV, the μ_X and σ_X as a function of μ_k and σ_k, the value of these variables are acquired by equating the two equations i.e. (3.7) and (3.8)

$$\widehat{\Psi}_{\phi}(s;\mu_X,\sigma_X) = \prod_{k=1}^{K} \widehat{\Psi}_{\nu_k}(s_i;\mu_k,\sigma_k,\kappa_k), \text{at } i = 1 \text{ and } 2. \tag{3.9}$$

The right hand side of the above equation consists of all the known elements, by solving for s_1 and s_2 we will only be left with unknown moments of X. The values for s_1 and s_2 are found by solving an optimization model

[31], $s_1 = 0.2$ is used to calculate the μ_X and $s_2 = 1.0$ for σ_X. Note that this method leaves us with two non-linear equations, which can be solved by using the standard fsolve function in MATLAB. Since the sum of K lognormal-Rice RVs are approximated by a single lognormal RV, the calculated μ_X and σ_X will give us the resultant lognormal RV.

Now to find that a node has decoded the message correctly, implies that, the received SNR is greater than or equal to a decoding threshold, τ. Hence we shape our conditional probability in (3.5) accordingly. At node k, the SNR received is determined by the distribution of RV ϕ, $\phi^{(k)} = 10^{0.1X^{(k)}}$, (3.5) becomes

$$\begin{aligned}\mathbb{P}_r\{\gamma_k(n) > \tau|\varepsilon\} = \mathbb{P}_r\{\phi^{(k)} > \tau|\varepsilon\} = \mathbb{P}_r\{10^{0.1X^{(k)}} \geq \tau\} = \\ \mathbb{P}_r\{X^{(k)} \geq 10\log\tau\} = Q\Big(\frac{10\log\tau - \mu_{X^{(k)}}}{\sigma_{X^{(k)}}}\Big).\end{aligned} \tag{3.10}$$

Therefore, the success probability depends upon the calculated μ_X and σ_X from (3.9) and τ. In a certain state, the one-hop probability is given by the product between probabilities of nodes that are in coverage multiplied with the probabilities of nodes that are in outage. If $\mathbb{N}_n^{(j)}$ is the set of indices of nodes that has decoded at time n being in state j and $\bar{\mathbb{N}}_n^{(j)}$ is a set for nodes that do not decode, then the one-step transition probability going from state i to j is given by

$$\begin{aligned}\mathbb{P}_{ij} = \prod_{k\in\mathbb{N}_n^{(j)}} Q\Big(\frac{10\log\tau - \mu_{X^{(k)}}}{\sigma_{X^{(k)}}}\Big)\times \\ \prod_{k\in\bar{\mathbb{N}}_n^{(j)}} \Big\{1 - Q\Big(\frac{10\log\tau - \mu_{X^{(k)}}}{\sigma_{X^{(k)}}}\Big)\Big\}.\end{aligned} \tag{3.11}$$

Chapter 4

Lognormal-Rice Fading with Random Path loss

In this chapter, we propose a geometric model for a 2-dimensional (2D) strip-shaped OLA network where each node broadcasts the message by using decode-and-forward (DF) technique, whereas, the wireless channel undergoes lognormal shadowing and Rice fading. Our 2-dimensional network comprises of hypothetical adjacent square regions with each region comprising of known number of randomly placed nodes. It is different from a typical OLA network in which irregular boundaries are formed by a group of nodes that increases the geometric complexity. The reason for this formation of 2-dimensional strip-shaped network is that, nodes of two neighbouring regions form a disjoint set [20, 22]. The fixed boundary confines the transmission from nodes only to the adjacent region. We can see implication of such layout in corridors having neighbouring rooms, or a vehicular network on a highway.

We model the process of transmission between a set of nodes transmitting the same message signal to another set of nodes as a discrete-time Markov

chain. The probability of a node to successfully decode the received message signal in a certain region given that at least one node transmitted in previous region is same for all the nodes of that particular region. At a particular node, the received signal is a sum of multiple transmitted signals received over orthogonal channels [30]. We assume that the transmit power of all the nodes are same and correct decoding occurs when node's received power after post-detection combining is greater than a defined threshold.

Our contributions include the derivation of the probability density function (PDF) of SNR at a node, which is a stochastic process that includes a ratio distribution of a lognormal random variable (RV) and random distance RV, along with Rice fading. The effect on network's coverage area is quantified as a function of path loss exponent, Rice K-factor and standard deviation of shadowing.

4.1 System Model

We describe the network layout and present an expression to compute the received power. An extended strip-shaped network is considered where each hop or level is a square region of area $\mathbb{A}$ such that $\mathbb{A} = L \times L$. Each level contains N randomly placed points as shown in Fig. 4.1. Let Γ denotes the point process on the bounded set $\mathbb{A}$, $\mathbb{A} \in \Re^2$, where $\Gamma(\mathbb{A}) = N$ with probability 1, such that the placement of nodes in $\mathbb{A}$ is random with a uniform distribution. S trip-shaped networks are widely used in many works studying cooperative communication between sender and receiver nodes ([**?**, 32] and references therein). The wireless propagations are considered to be impacted by three channel impairments; path loss between randomly distributed nodes,

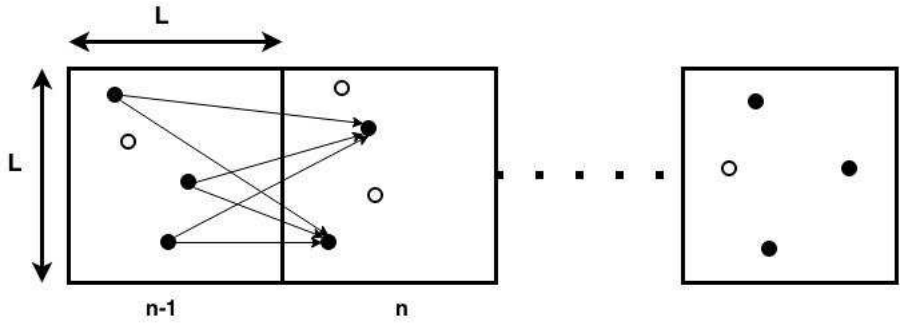

Figure 4.1: Illustration of geometric strip-shaped network for $N = 4$

large-scale shadowing and small-scale fading.

At each level, the N nodes form an OLA, cooperating synchronously to transmit the same message to the nodes in the next level using a decode-and-forward (DF) method. However, for a node to successfully decode the message signal, the received signal-to-noise ratio (SNR) should be greater than or equal to a defined decoding threshold, τ. As illustrated in Fig. 4.1, the nodes that are not able to decode are shown hollow whereas the nodes filled in black are those that decoded correctly.

The received power, P_{r_m}, at any node m at a level n in the network can be represented by

$$P_{r_m}(n) = \sum_{k \in \mathcal{M}_{n-1}} \frac{P_t \nu_{mk}}{(d_{mk})^{\beta}}. \tag{4.1}$$

In the above equation, P_t, is transmit power and ν_{mk} is a coefficient for composite fading that represents the small-scale as well as large-scale channel fading between a node k at level $n-1$ and a node m at level n. Let $\mathcal{M}_{n-1}$ be the set of DF nodes at level $n-1$, where the cardinality of the set $\mathcal{M}_{n-1}$ is always less than or equal to N, i.e., $|\mathcal{M}_{n-1}| \leq N$. We model the large-scale fading or shadowing as a lognormal random variable (RV) and small-scale

fading is modeled by a Rice RV. The d_{mk} is the Euclidean distance between the node k at level $n-1$ and node m at level n and β is the path loss exponent.

4.2 Propagation Model

In this section, we model the hop-transmissions in the network by using Markov chains. Successful transmissions are assumed if a node's received power is greater than or equal to a defined decoding threshold, τ. We define $\mathbb{I}_j(n)$ as a binary RV reflecting the state of j^{th} node at level n. This implies that a node can either be in state 1, if it decodes the data properly, and state 0 if it does not decode the data. At a particular level containing N nodes, the binary indicator functions of all the nodes can be combined to constitute a single state, which represents the state of the system for that level. For example at a level n, if N=4 and only one node has decoded the data, then possible system states could be $[1000], [0100], [0010], [0001]$. This is because the nodes are randomly placed and not tagged. Therefore, we denote the state of a particular hop n based upon the number of DF nodes in a level, i.e., $\mathcal{Y}(n) = \sum_{j=1}^{N} \mathbb{I}_j(n)$. Furthermore, notice that node participation depends on the condition that at least one node at level $n-1$ has transmitted, hence $\mathcal{Y}(n)$ depends only on $\mathcal{Y}(n-1)$ making $\mathcal{Y}$ a finite state Markov chain. Moreover, there can be a possibility where no node in a level decodes, the point where Markov chain enters the absorbing state, $\{0\}$, resulting in no further propagations. Thus $\mathcal{Y}(n)$ can be defined as a homogeneous finite state Markov chain, defined on two sets, i.e., $\mathcal{Y}(n) \in \{0\} \cup \mathbf{S}$ where $\mathbf{S}$ is the

irreducible state space given as,

$$\mathbf{S} = \begin{cases} 1 & \text{Precisely one node decodes} \\ 2 & \text{Precisely two nodes decode} \\ \vdots & \\ N & \text{Precisely all nodes decode} \end{cases} . \tag{4.2}$$

We also assume that the channel statistics remain the same and synchronous transmission occurs at every distinct time slot with each node having equal transmit power. This Markov chain can be defined by an $(N+1) \times (N+1)$ dimensional transition probability matrix, $\tilde{\mathbf{T}}$. However, we are only interested in finding the state of the system just before the transmission stops. By removing the first column and first row of the matrix, transitions to and from absorbing state reduces $\tilde{\mathbf{T}}$ to $N \times N$ dimension, forming a new sub-matrix, $\mathbf{T}$, which is an irreducible square matrix with non-negative entries and state space $\mathbf{S}$. According to Perron-Frobenius theorem [34], there exists a unique maximum eigenvalue, ρ, and a unique eigenvector, $\mathbf{v}$, for the matrix $\mathbf{T}$ such that $\mathbf{vT} = \rho\mathbf{v}$. The elimination of state 0 makes $\mathbf{T}$ a right sub-stochastic matrix, i.e., the value of Perron eigenvalue will always be less than unity. The state distribution of the system before going into killing (absorbing) state is called the quasi-stationary distribution, if $\mathbf{v}$ is the left eigenvector of matrix, $\mathbf{T}$, then $\mathbf{v} = (v_i, i \in \mathbf{S})$ is the ρ-invariant distribution. Hence quasi-stationary distribution for the Markov chain at any state i becomes,

$$\mathbb{P}\{\mathcal{Y}(n) = i | \mathcal{K} > n\} = v_i, i \in \mathbf{S}, \quad \forall n \quad , \tag{4.3}$$

where, $\mathcal{K} = inf\{n \geq 0 : \mathcal{Y}(n) = 0\}$ is the event of absorbing state. The

probability of being in state, i, at a certain level n, can be calculated as

$$\mathbb{P}\{\mathcal{Y}(n) = i\} = \rho^n v_i, i \in \mathbf{S}, n \geq 0 \quad . \tag{4.4}$$

4.3 Formulation of the Transition Matrix for Random Path loss Network

At one hop, a node receives multiple message copies of the same signal under the impacts of multipath fading, shadowing and path loss. The received SNR at the i^{th} node at level n is given by $\gamma_i(n) = P_{r_i}(n)/\sigma_N^2$, where, P_{r_i} is the received power as given in (4.1) and σ_N^2 is the white noise. For node i to successfully decode a message signal at time n,

$$\begin{aligned} P_s = \mathbb{P}\{\text{Success of node i}|\varepsilon\} = \mathbb{P}\{\mathbb{I}_i(n) = 1|\varepsilon\} = \\ \mathbb{P}\{\gamma_i(n) > \tau|\varepsilon\} = \int_\tau^\infty p_{\gamma_i|\varepsilon}(z)\,\mathrm{d}z \quad , \end{aligned} \tag{4.5}$$

where $p_{\gamma_i|\varepsilon}(z)$ is the conditional PDF of the received SNR, conditioned on the previous state $\varepsilon \in \mathbf{S}$, and P_o is the outage probability, where $P_o = 1 - P_s$. Notice that for a certain number of transmitting nodes, i.e., $|\mathcal{M}_{n-1}|$, and constant network conditions, i.e., transmit power, P_t, path loss exponent, β, and L region length, the success probability for all the nodes of a particular level remains the same. This is because the distance between nodes and fading gains are both random. Having said that, the conditional probability of transition from state s_1 to another state s_2, for $s_1, s_2 \in \mathbf{S}$, can be found

by using the binomial theorem, i.e.,

$$\mathbb{P}(s_1|s_2) = \begin{pmatrix} N \\ s_2 \end{pmatrix} P_s^{s_2} (P_o)^{N-s_2}, \tag{4.6}$$

where P_s is as defined in (4.5). We now proceed to find the outage (or success) probability of a node at an arbitrary state. From (4.1), we can see that the received power at a node is a stochastic process that includes three RVs, namely, random distance, shadowing and fading. If we define Θ to be a RV that encompasses all these effects, then Θ can be given as,

$$\Theta = \frac{XR}{W}, \tag{4.7}$$

where RV X defines lognormal shadowing, R denotes the multipath fading and W is the RV used to denote the Euclidean distance between two nodes. It was shown in [27] that the random distance between a pair of nodes, when nodes are placed in adjacent square region can be approximated by a Weibull RV. The distribution of the Euclidean distance raised to any power β is given by

$$f_W(w) \approxeq \frac{c}{\chi^c} w^{c-1} \exp^{-(\frac{w}{\chi})^c}, \tag{4.8}$$

where $c = 2p/\beta$ is the shape parameter and $\chi = \lambda^p$, for $\lambda = 4L^2/(3\Gamma(1.6327))$, is the scale parameter of Weibull distribution with constant $p = 1.5806$. Here L is the length of the square region. The following sequence of work is now used to find the PDF of RV defined by (4.7). At first we compute the PDF of the ratio of lognormal RV, X, and Weibull RV, W, using the product distribution between lognormal and Inverse Weibull distribution. We then compute another product distribution to find the PDF of RV in (4.7).

Let $W \sim Weibull(c, \chi)$ then $Y = 1/W$ is the $InvWeibull(\alpha, \aleph)$, where the inverse Weibull distribution is given by

$$f_Y(y) = \frac{\alpha}{\aleph^\alpha} y^{-\alpha-1} \exp^{-(\aleph y)^{-\alpha}}, \tag{4.9}$$

where the scale and shape parameters are same as that of Weibull distribution. We now find the product distribution of lognormal and inverse Weibull RVs using the following lemma.

Lemma 1. *The product of an Inverse Weibull RV, Y, and a lognormal RV, X, can be approximated by another lognormal RV, Z with mean $\mu_Z = \frac{1}{\zeta}(\frac{C}{\alpha} - \ln \aleph) + \mu_X(dB)$ and variance $\sigma_Z^2 = \frac{\pi^2}{6\zeta^2\alpha^2} + \sigma_X^2$, where $C = 0.5772$ and $\zeta = \ln(10)/10$, μ_X and σ_X^2 are the mean and variance of X while α and $\aleph$ are the scale and shape parameters of Y.*

Proof. The distribution of a product RV $Z = XY$ is generally given by

$$p_Z(z) = \int_{-\infty}^{\infty} \frac{1}{|x|} f_X(x) f_Y\left(\frac{z}{x}\right) \mathrm{d}x. \tag{4.10}$$

The PDF of the product of lognormal and inverse Weibull RV can thus be expressed by the following equation.

$$\begin{aligned} p_Z(z) = \frac{\alpha}{\zeta \aleph^\alpha \sigma_X \sqrt{2\pi}} \int_0^\infty \frac{1}{x^2} \left(\frac{x}{z}\right)^{\alpha+1} \exp\left\{ -\left(\frac{x\aleph}{z}\right)^\alpha \right\} \\ \times \exp\left\{ \frac{-(10\log_{10}(x) - \mu_{X_{(dB)}})^2}{2\sigma_{X_{(dB)}}^2} \right\} \mathrm{d}x. \quad . \end{aligned} \tag{4.11}$$

It can be noticed that the product distribution does not exist in a closed-form. Hence we use the moment matching technique to calculate the moments of approximating lognormal RV, $Z = 10^{\frac{\phi}{10}}$ such that $\phi \sim \mathcal{N}(\mu_\phi, \sigma_\phi^2)$

and $Z \sim Log\mathcal{N}(\mu_\phi, \sigma_\phi^2)$. Since Z is lognormal, therefore, the computation of first two moments is sufficient. To extract the mean and variance from (4.11) consider finding the first moment of the associated normal RV, i.e.,

$$\mu_\phi = \mathbb{E}[10\log_{10} Z] = \frac{\alpha}{\zeta \aleph^\alpha \sigma_X \sqrt{2\pi}} \int_0^\infty 10\log_{10}(z) \times \int_0^\infty \exp\Big\{-\Big(\frac{x\aleph}{z}\Big)^\alpha\Big\} \exp\Big\{\frac{-(10\log_{10}(x) - \mu_{X_{(dB)}})^2}{2\sigma_X^2}\Big\} \mathrm{d}z\mathrm{d}x. \tag{4.12}$$

Solving the equation with respect to the inner integral, we obtain,

$$\mathbb{E}[10\log_{10} Z] = -\frac{1}{\alpha\sigma_X\sqrt{2\pi}} \int_0^\infty \frac{1}{x}\Big(C + \ln\Big(\frac{\aleph}{x}\Big)^{-\alpha}\Big) \exp\Big\{\frac{-(w - \mu_{X_{(dB)}})^2}{2\sigma_X^2}\Big\} \mathrm{d}w. \tag{4.13}$$

By solving above equation with respect to $\mathrm{d}w$ gives us the first moment

$$\mu_\phi = \mathbb{E}[10\log_{10} Z] = \frac{1}{\zeta}\Big(\frac{C}{\alpha} - \ln\aleph\Big) + \mu_{X_{(dB)}}. \tag{4.14}$$

Where $C \backsimeq 0.5772$ is the Euler's constant. Using a similar approach for the second moment,

$$\mathbb{E}[(10\log_{10} Z)^2] = \frac{1}{6\zeta^2\alpha^2}\{6C^2 + \pi^2 - 12\alpha C\ln(\aleph) + 6\alpha^2(\ln(\aleph))^2\} + \frac{2\mu}{\alpha\zeta}\{C - \alpha\ln(\aleph)\} + \mu_{X_{(dB)}}^2 + \sigma_{X_{(dB)}}^2 \tag{4.15}$$

Hence, the variance of Z can be calculated by using (4.14) and (4.15) as,

$$\sigma_\phi^2 = \frac{\pi^2}{6\zeta^2\alpha^2} + \sigma_{X_{(dB)}}^2. \tag{4.16}$$

□

In Lemma 1, we can see that the random inter-nodal distance and log-normal shadowing are now approximated with a single lognormal RV with

certain mean and variance. Therefore, Equation (4.7) is now reduced to $\Theta \cong ZR$, where Z is a lognormal RV with mean as in (4.14), and variance, as in (4.16), and R is the Ricean RV with Rice factor κ. Next, we approximate the lognormal-Rice product distribution by another lognormal RV, $U = 10^{\frac{G}{10}}$, where G is associated normal RV, however, the closed-form PDF for their product is also prohibited. For this approximation, one method is to use the moment matching technique as shown in Lemma 1, or the other method is to use the moment generating function (MGF) method. We use the latter approach.

In MGF-based method, the MGF of the approximating lognormal RV, U, and the MGF of the lognormal-Rice RVs, ZR, is equated at two distinct points to find the mean and variance of U. Whereas, it is difficult to find the MGF in closed-form, however, by applying Gauss-Hermite integration these can be computed. In Gauss-Hermite integration, the integral is estimated by an approximate sum where the summation is defined by specific weights.

The PDF of the approximating lognormal RV, U, can be expressed as

$$p_U(u) = \int_{-\infty}^{\infty} \frac{\zeta}{u\sigma_{G_{(dB)}}\sqrt{2\pi}} \exp\left\{\frac{-(\zeta \log_e u - \mu_{G_{(dB)}})^2}{2\sigma^2_{G_{(dB)}}}\right\} \mathrm{d}u, \tag{4.17}$$

where $\mu_{G_{(dB)}}$ and $\sigma^2_{G_{(dB)}}$ is the mean and variance of the associated Gaussian RV, G, respectively. The MGF of U is given by

$$\Psi_U(s) = \int_0^{\infty} \exp(-su) p_U(u) \mathrm{d}u, \tag{4.18}$$

After substitution, (4.18) can be re-written as

$$\Psi_U(s) = \int_{-\infty}^{\infty} \frac{1}{\sqrt{\pi}} \exp(-r^2) \left[- s \exp\left(\frac{\sqrt{2}\sigma_{G_{(dB)}} r + \mu_{G_{(dB)}}}{\xi} \right) \right] \mathrm{d}u, \tag{4.19}$$

where $r = \frac{\zeta \log_e u - \mu_{G_{(dB)}}}{\sqrt{2}\sigma_{G_{(dB)}}}$. The MGF in the above integral form cannot be computed analytically, however, it can be seen that this form of equation is the well-known Hermite polynomial, which can be computed by applying Gauss-Hermite integration as

$$\Psi_U(s; \mu_{G_{(dB)}}, \sigma_{G_{(dB)}}) = \sum_{h=1}^{H} \frac{w_h}{\sqrt{\pi}} \exp\left[- s \exp\left(\frac{\sqrt{2}\sigma_{G_{(dB)}} a_h + \mu_{G_{(dB)}}}{\xi} \right) \right], \tag{4.20}$$

where Hermite integration order, H, is used to achieve better estimation of the MGF of U; the larger the value of H the better the estimate. The w_h is the weight corresponding to the abscissas, a_h, and $\xi = 10/\ln 10$, is a constant for scaling. In [36], weights, abscissas and the values for H can be found in a tabulated form. Similarly, the PDF of lognormal-Rice RV, $\Theta = ZR$, where Z is the lognormal RV with mean μ_ϕ and variance σ_ϕ^2 and R is the Ricean RV with Rice-factor κ takes the integral form

$$\begin{aligned} p_\Theta(\theta) = \int_0^\infty \frac{2\theta(\kappa+1)}{z^2} \exp\left\{ - \kappa - (\kappa+1)\frac{\theta}{z^2} \right\} \\ \times I_0\left(\frac{2\theta}{z}\sqrt{\kappa(\kappa+1)} \right) p_Z(z) \mathrm{d}z \quad , \end{aligned} \tag{4.21}$$

where I_0 is the modified Bessel function of zero order and $p_Z(z)$ is given in (4.11). The MGF of the lognormal-Rice RV, Θ, after applying Gauss-Hermite integration, can be written as

$$\begin{aligned} \Psi_\Theta(s; \mu_\phi, \sigma_\phi, \kappa) = \sum_{h=1}^{H} \frac{w_h(1+\kappa_R)/\sqrt{\pi}}{1 + \kappa_R + s\exp(\frac{\sqrt{2}\sigma_\phi a_h + \mu_\phi}{\xi})} \\ \times \exp\left(- \frac{s\kappa_R \exp(\frac{\sqrt{2}\sigma_\phi a_h + \mu_\phi}{\xi})}{1 + \kappa_R + s\exp(\frac{\sqrt{2}\sigma_\phi a_h + \mu_\phi}{\xi})} \right) \quad . \end{aligned} \tag{4.22}$$

The mean and variance parameters, $\mu_{G_{(dB)}}$ and $\sigma^2_{G_{(dB)}}$, of the approximated lognormal RV can be calculated by equating (4.20) and (4.22) as,

$$\Psi_U(s_i; \mu_{G_{(dB)}}, \sigma_{G_{(dB)}}) = \Psi_\Theta(s_i; \mu_\phi, \sigma_\phi, \kappa) \qquad i = 1 \text{ and } 2. \tag{4.23}$$

The two non-linear equations can be solved using a numerical routine. As the right-hand side comprises of all known variables, solving for s_1 and s_2 we get the desire moments of U. Hence, we can say that the impact of three RVs on a single path of transmission can be approximated with a single lognormal RV. We now focus on a more general arrangement where multiple nodes are transmitting the same message to a node at the next level. In this case, the received power is the sum of RVs from all different transmission paths, each following independent distribution due to distinct σ of each RV. If $A = |\mathcal{M}_{n-1}|$ is the number of DF nodes at level $n-1$ then

$$\sum_{\ell=1}^{A}\{\Theta_\ell\} = \sum_{\ell=1}^{A}\left\{\frac{X_\ell R_\ell}{W_\ell}\right\}. \tag{4.24}$$

As each Θ is approximated as a lognormal RV, U, the received power at a node at level n is the sum of A independent but non-identical lognormal RVs. We again use the MGF transformation method here as the distribution for sum of lognormal RVs does not exist in a closed-form, [31]. In MGF domain, the summation of RVs are represented as the product of their individual MGFs. The MGF for the sum of lognormal RVs, $\sum_{\ell=1}^{A} U_\ell = (U_1, U_2, \ldots, U_A)$, is given as,

$$\sum_{\ell=1}^{A} \Psi_{U_\ell}(s_i; \mu_{G^{(\ell)}_{(dB)}}, \sigma_{G^{(\ell)}_{(dB)}}) = \prod_{\ell=1}^{A} \Psi_{U_\ell}(s_i; \mu_\ell, \sigma_\ell) \quad i = 1 \text{ and } 2 \tag{4.25}$$

where $\mu_{G^{(\ell)}_{(dB)}}, \sigma_{G^{(\ell)}_{(dB)}}$ is the mean and standard deviation of each individual lognormal RV, U. Furthermore, by using (4.23) we can rewrite (4.25) as

$$\sum_{\ell=1}^{A} \Psi_{U_\ell}(s_i; \mu_{G^{(\ell)}_{(dB)}}, \sigma_{G^{(\ell)}_{(dB)}}) = \prod_{\ell=1}^{A} \Psi_{\Theta_\ell}(s_i; \mu_\ell, \sigma_\ell, \kappa_\ell) \quad i = 1 \text{ and } 2 \tag{4.26}$$

where μ_ℓ and σ_ℓ are the mean and standard deviation of the A^{th} lognormal-Rice RV, Θ and κ_ℓ is the Rice-factor. Therefore, we can approximate sum of A lognormal-Rice RVs, $\{U_1, U_2, \ldots, U_A\}$, by a single lognormal RV, $\mathcal{J} = 10^{\frac{\mathcal{L}}{10}}$ such that $\mathcal{J} \sim Log\mathcal{N}(\mu_\mathcal{L}, \sigma^2_\mathcal{L})$. The approximated single lognormal RV $\mathcal{J}$'s MGF is given by,

$$\Psi_\mathcal{J}(s; \mu_\mathcal{L}, \sigma_\mathcal{L}) = \sum_{h=1}^{H} \frac{w_h}{\sqrt{\pi}} \exp\left[- s \exp\left(\frac{\sqrt{2}\sigma_\mathcal{L} a_h + \mu_\mathcal{L}}{\xi} \right) \right]. \tag{4.27}$$

Hence, by using (4.26) and (4.27) we can get,

$$\begin{aligned} \sum_{h=1}^{H} \frac{w_h}{\sqrt{\pi}} \exp\left[- s_i \exp\left(\frac{\sqrt{2}\sigma_\mathcal{L} a_h + \mu_\mathcal{L}}{\xi} \right) \right] = \\ \prod_{\ell=1}^{A} \sum_{h=1}^{H} \frac{w_h(1+\kappa_\ell)/\sqrt{\pi}}{1 + \kappa_\ell + s_i \exp(\frac{\sqrt{2}\sigma_\ell a_h + \mu_\ell}{\xi})} \quad i = 1 \text{ and } 2.. \\ \times \exp\left(- \frac{s_i \kappa_\ell \exp(\frac{\sqrt{2}\sigma_\ell a_h + \mu_\ell}{\xi})}{1 + \kappa_\ell + s_i \exp(\frac{\sqrt{2}\sigma_\ell a_h + \mu_\ell}{\xi})} \right) \quad . \end{aligned} \tag{4.28}$$

Here $\mu_\mathcal{L}$ and $\sigma^2_\mathcal{L}$ is the logarithmic mean and variance of lognormal RV $\mathcal{J}$. It can be noticed that out of the two non-linear equations in (4.28), the right-hand side contains of all known quantities, and can be solved as previously.

After deriving the PDF of RVs, we now concentrate to derive the success probability of a node in Fig. 4.1. To find that a node has decoded the

message correctly, the received SNR should be greater than or equal to a decoding threshold, τ. To be specific, the received SNR of a node i at level n is determined by the distribution of RV $\mathcal{J}$, now given as,

$$\gamma_i(n) = \frac{P_t}{\sigma_N^2} \sum_{\ell=1}^{A} \{\Theta_\ell\} = \frac{P_t}{\sigma_N^2} \mathcal{J}^{(i)}. \tag{4.29}$$

This alters the conditional probability in (4.5) as

$$\begin{aligned} \mathbb{P}\{\gamma_i(n) > \tau|\varepsilon\} = \mathbb{P}\Big\{ \frac{P_t}{\sigma_N^2} \mathcal{J}^{(i)} > \tau|\varepsilon \Big\} = \mathbb{P}\Big\{ \frac{P_t}{\sigma_N^2} 10^{\frac{\mathcal{L}^{(i)}}{10}} \geq \tau \Big\} = \\ \mathbb{P}\Big\{ \mathcal{L}^{(i)} \geq 10 \log\Big(\frac{\sigma_N^2 \tau}{P_t} \Big) \Big\} = Q\Big(\frac{10 \log(\sigma_N^2 \tau / P_t) - \mu_{\mathcal{L}^{(i)}}}{\sigma_{\mathcal{L}^{(i)}}} \Big), \end{aligned} \tag{4.30}$$

where Q-function denotes the tail probability, which is of our interest in determining the outage probability. It is important to notice that the success probability depends on the transimit power, P_t, decoding threshold, τ, and calculated $\mu_{\mathcal{L}}$ and $\sigma_{\mathcal{L}}$ from (4.28). In a certain state, the one-hop probability is given by (4.6) and the nodes probability to decode or not is given by (4.30). Similarly, for all nodes in level n the same method is repeated which will populate our transition probability matrix, $\mathbf{T}$. The Perron-Frobenius theorem is then applied on $\mathbf{T}$ to determine the one-hop success probability. Our work flow in this chapter can be logged as shown in Table 4.1.

Table 4.1: Work flow of deriving the PDF of SNR at a node.

Expression	Transformation	Process	Method used
$\Theta = \frac{XR}{W}$	$W = \frac{1}{Y}$	W Weibull RV is transformed into Inverse Weibull RVY	Variable transformation
	$Z = XY$	The product distribution; in Lemma 1	Moment matching approach
	$\Theta = ZR$	The product distribution	MGF-based method
	$\Psi_U(s; \mu_{G_{(dB)}}, \sigma_{G_{(dB)}})$ $= \Psi_\Theta(s; \mu_\phi, \sigma_\phi, \kappa_R)$	lognormal-Rice RV approximation	MGF-based method
$\sum_{i=1}^{A}\{\Theta_i\}$ $= \sum_{i=1}^{A}\left\{\frac{X_i R_i}{W_i}\right\}$	$\sum_{i=1}^{A}\{\Theta_i\}$	Sum of A lognormal RVs	MGF-based approach
	$\sum_{i=1}^{A}\{U_i\}$ $= \prod_{\ell=1}^{A}\Psi_{\Theta_\ell}(s_i; \mu_\ell, \sigma_\ell)$	The sum into product conversion	MGF-based approach
	$\mathcal{J} = \sum_{i=1}^{A}\{U_i\}$	Sum approximation as a single lognormal RV$\mathcal{J}$	MGF-based approach
	$\mathcal{J} = \prod_{\ell=1}^{A}\Psi_{\Theta_\ell}(s_i; \mu_\ell, \sigma_\ell, \kappa_\ell)$	The final lognormal RV as a product of A lognormal-Rice RVs	MGF-based approach
Received SNR at a node i	$\gamma_i(n) = \frac{P_i}{\sigma_N^2}\mathcal{J}^{(i)}$		

Chapter 5

Results and System Performance

In this section, we present some numerical results for various sets of parameters. We carried out numerical simulations to validate analytical models derived in the previous section.

5.1 Deterministic Network Results

For the simulation environment, we consider M number of nodes in a level with some initial distribution of DF nodes for the first hop. The Euclidean distance between the current hop and the next hop nodes is computed. The received power is calculated at each node, which in turn sets the indicator function to either 0 or 1. The new state distribution for the current hop is checked for an absorbing state (i.e. none of the node is able to decode) and the process continues.

The case of composite Rician and lognormal fading channel is catered by

generating these processes separately and then multiplying them together. The important parameters to handle are the K-factor of Rice distribution and the mean and standard deviation of shadowing. We obtained one-hop success probability, ρ, for both simulations and analytical model. In the case of simulations, ρ is the probability that at least one node in a level decodes the message successfully and we averaged out these simulations over 1 million trials. For illustration, the results are taken for a certain normalized SNR at each node, called the SNR margin, $\Upsilon = \frac{P_t}{\tau d^{\beta}}$. We assume $d = 1$ and $P_t = 1$ for all results and the path loss exponent, $\beta = 2$, is used unless mentioned otherwise. The length and width of the level are kept fixed at $L = 3$ and $W = 2$ until otherwise stated.

From Fig. 5.1, it is obvious that both the analytical and the simulation results are quite close to each other, which verify the accuracy of the proposed analytical model. As the SNR margin increases, the probability of being in a transient state also increases, which increases the probability for more number of nodes to decode in a certain level.

Fig. 5.2 shows the one-hop success probability for different parameters of shadowing and fading, at various SNR margins. It can be seen that as the SNR margin increases the probability of one-hop success also increases, which is intuitive because of an increased transmit power and/or reduced distance and threshold. In Fig. 5.2, we get two important notions depicting the behaviour of success as a function of σ. It can be observed that for low SNR margins, i.e., $\Upsilon \leq 9$dB, an increase in σ results in an increase in ρ. This seems contradictory because an increase in σ depicts the severity of shadowing. In a wireless channel, σ depicts the variation in the received power across a

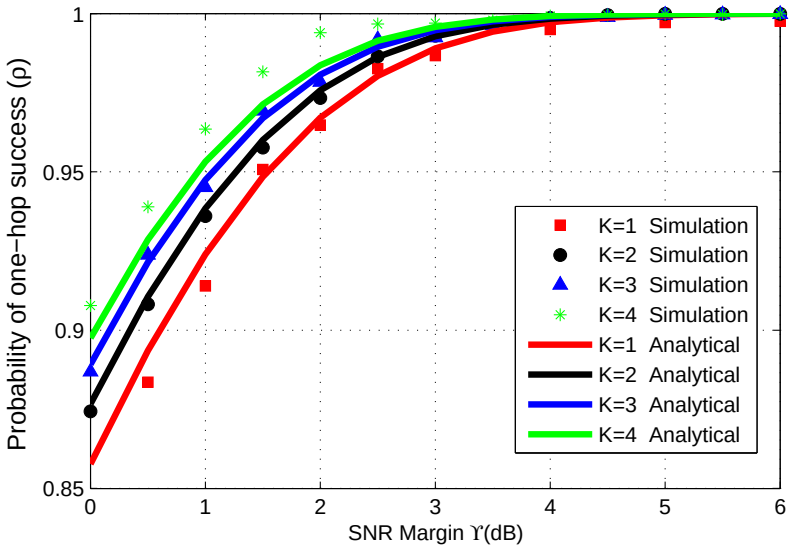

Figure 5.1: Simulation versus analytical results, $M = 6, \sigma = 10$

certain mean and the mean in turn defines the path loss exponent; the larger the σ, the higher the variations. At low SNR margins, the only nodes present at the tail of a level will actively take part in transmission to the next hop due to minimum path loss between them and the next level nodes as compared to the nodes, which are at the starting edge with relatively higher path loss. Therefore, on low SNR margins, when path loss is high, we can get a favourable response when σ is increased, which eventually increases the one-hop success probability. As the SNR margin attains higher values, the path loss decreases and only the severity of shadowing causes the probability of success to drop for large values of σ, as shown in the zoomed portion of Fig. 5.2, where the behaviour of curves is reversed.

Also note that the effect of path loss, at a particular σ, suppresses the effect of K-factor. When we increase K for a certain σ, the probability of

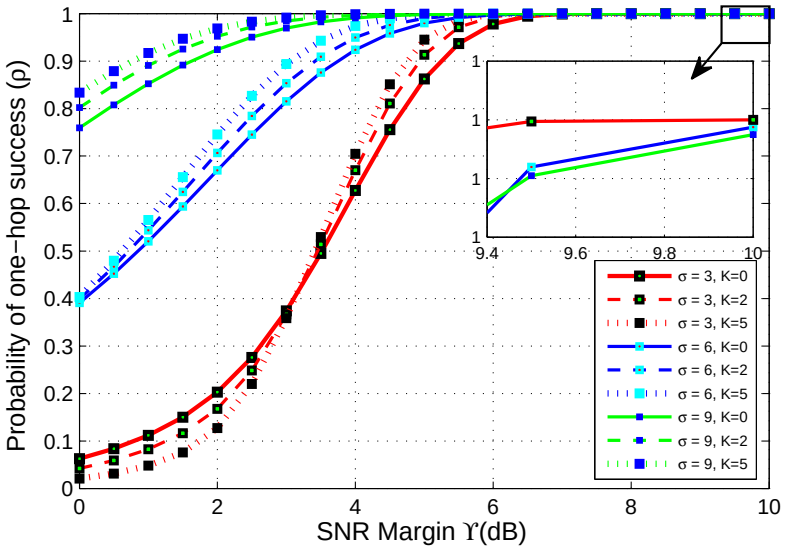

Figure 5.2: Success probability vs. SNR margin for $L = 3, W = 2; M = 6, \beta = 2$

one-hop success decreases for low values of SNR margin. However, increase in K-factor reduces the occurrence of fade and act as a gain factor in the received signal but the signal becomes more vulnerable to the fact that only few number of nodes are actively cooperating in transmission because of higher path loss, which decrease the success probability. The increase in the SNR margin reduces the path loss and we get better one-hop probability for large values of K. Furthermore, to see more clearly the effect of path loss exponent in the presence of shadowing and fading, we acquired results for different deployment of nodes, $L = 2$ and $W = 3$, as shown in Fig. 5.3. It can be seen that even for low SNR margins we have better one-hop success probability as compared to the case where we have two nodes at the tailing end.

In Fig. 5.4 we show results for different K-factors at various SNR margins

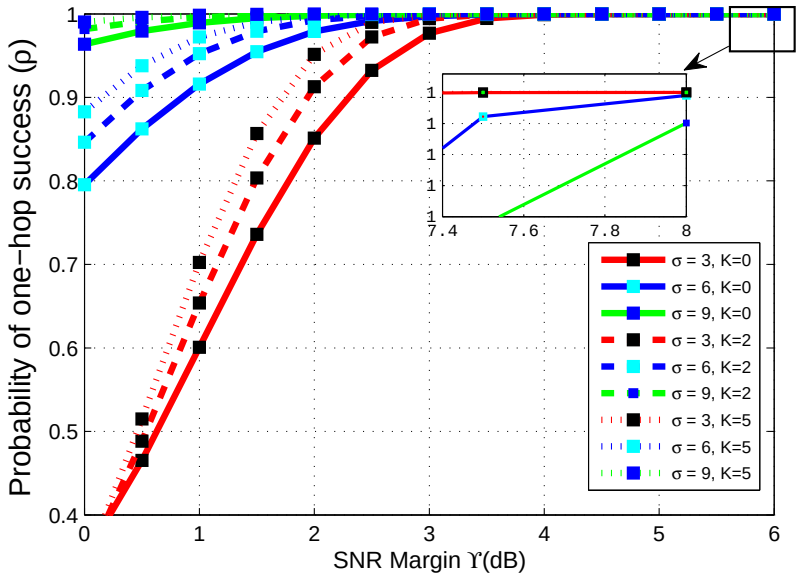

Figure 5.3: Success probability vs. SNR margin for $L = 2, W = 3; M = 6, \beta = 2$

by keeping $\sigma = 10dB$. For a particular value of SNR margin, as we increase the value of K the probability of one-hop success also increases. This shows that for K=0, when there is no LOS component in our received signal, we need more SNR margin to reach same ρ as compared to higher values of K. Also the increase in path loss exponent, β, from 2 to 3 requires almost 5dB more SNR margin for the same value of K.

To enhance the performance of the network we need to control certain parameter like distance between nodes and their transmit power. The probability of end-to-end successful delivery of a message without going into absorbing state is defined by a certain quality of service (QoS) parameter, η i.e. if we need to reach a certain distance with 90% QoS then $\eta \cong 0.9$. Since we know that, the propagation of a message for the maximum number of

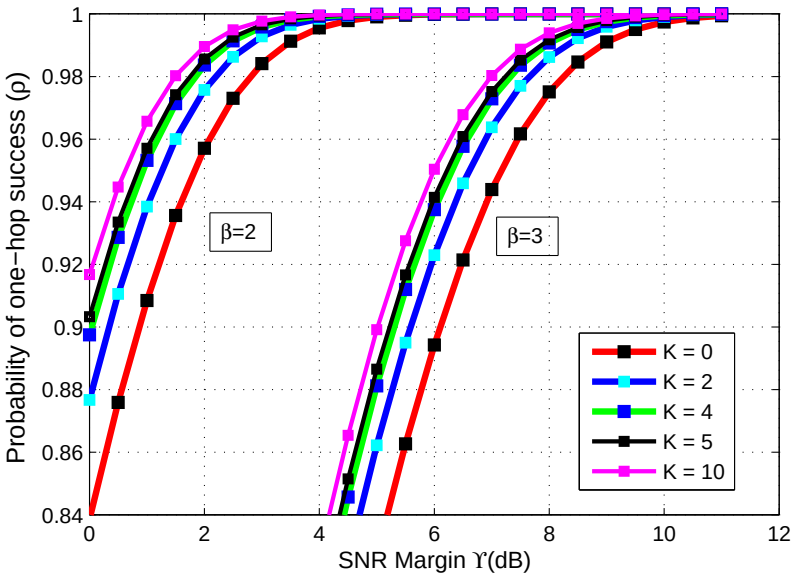

Figure 5.4: Success probability for different value of K-factor

hops, h, until the killing occurs is given by, ρ^h. So maximum value of hop count is bounded, i.e., $\rho^h \geq \eta$, which gives the maximum number of hops as $h \geq \frac{\ln \eta}{\ln \rho}$. If we take the product of number of hops with the number of nodes in horizontal dimension, L, it will give us the coverage range or maximum distance a message can go with the QoS. In Fig. 5.5, the normalized number of hops versus SNR margin for the topology of nodes in Fig. 3.1, is shown for varying η. We can see that an increase in the value of η reduces the number of hops, which is quite intuitive as we increase the QoS for same SNR margin, the probability of successful delivery also reduces.

In Table 5.1, we quantify the coverage range for different arrangements of nodes while varying K-factor and keeping $\sigma = 10dB$ fixed for specific SNR margins of $\Upsilon = \{2, 5, 10\}dB$ to achieve a QoS of 90%. The cases considered are:

Table 5.1: Coverage range for different topologies at $\eta = 0.90$

K-factor	CASE	$\Upsilon = 2$	$\Upsilon = 5$	$\Upsilon = 10$
K=5	A	0	6	708
	B	4	7230	2.09e+09
	C	6726	1.07e+07	6.05e+13
	D	9.96e+06	8.02e+10	1.42e+15
K=10	A	0	6	1122
	B	60	1.38e+07	6.85e+09
	C	1.31e+04	2.89e+07	3.34e+14
	D	2.91e+07	3.54e+11	2.84e+15

CASE A $L = 6, W = 1$; CASE B $L = 3, W = 2$

CASE C $L = 2, W = 3$; CASE D $L = 1, W = 6$

Notice that as we increase the number of nodes at the tailing edge of the transmission window, we get a considerable increase in the maximum achievable distance, i.e., the message can propagate to far off destinations. Furthermore, it can be seen from Table 5.1 that an increase in K-factor also improves the coverage range of the network. However, in a 2-D context there is a trade off, as an increase in the vertical dimension require a large number of nodes to cover the same region as compared to topology of nodes with larger horizontal stretch. To achieve high reliability, one can go with the arrangement in CASE D, whereas, to improve the latency or propagation delay, the better choice is CASE A.

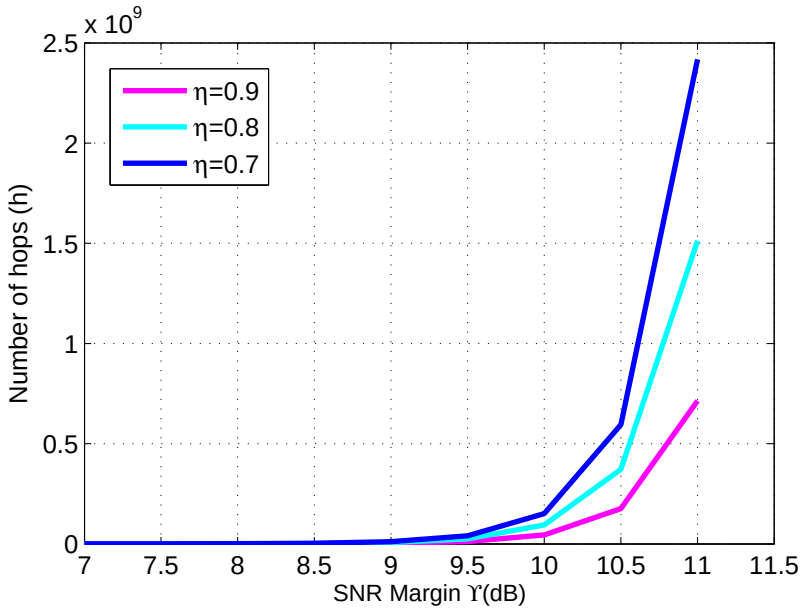

Figure 5.5: Number of hops for various value of η

5.2 Stochastic Network Results

In this section, we validate our analytical models for stochastic geometry of nodes and present some numerical results for various sets of parameters. At first we plot the comparison between the cumulative distribution function (CDF) of the approximated lognormal RV and network simulations to determine the accuracy of model proposed in Lemma 1. Monte-Carlo simulation of the product of lognormal and inverse Weibull RV is performed and compared with the proposed moment matching method. In simulation, the inverse Weibull and lognormal RVs are generated separately, multiplied and averaged over 10^7 iterations of Monte-Carlo. From Fig. 5.6, we can see that the CDF obtained for both the moment matching approach and network simulations is in a good match, hence, providing an accuracy of approximation proposed.

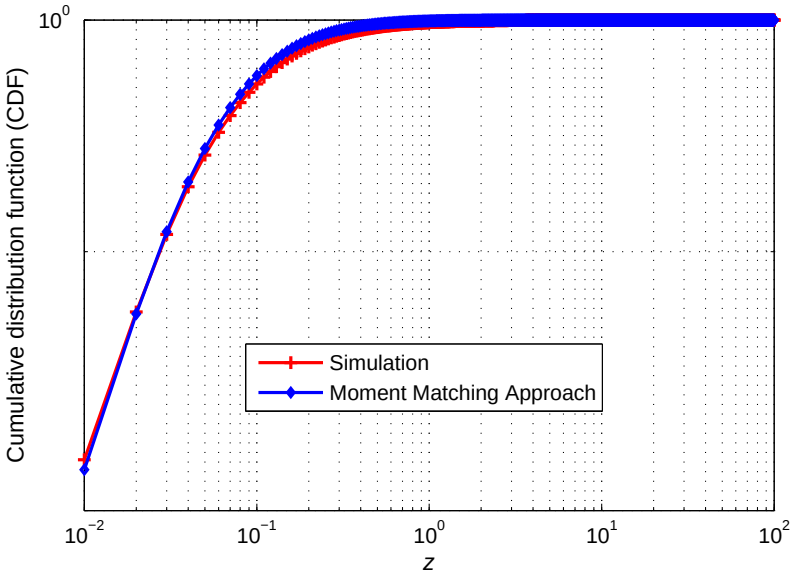

Figure 5.6: CDF comparison of theoretical and simulation approaches, $\beta = 2, L = 2, \mu_\phi = 0dB, \sigma_\phi = 6dB$,

Fig. 5.7 shows the one-hop success probability, ρ, for both analytical model and simulations, for 3 nodes in a level. The analytical values of one-hop success is the Perron-Frobenius eigenvalue obtained by forming the transition probability matrix, $\mathbf{T}$, where each value of $\mathbf{T}$ is evaluated using (4.6). On the other hand, for simulations, the one-hop success probability is calculated using the fact that at least one node in a level decodes the message signal correctly, where N nodes are randomly generated in adjacent square regions of $L = 5$. The normalized SNR margin, $\Upsilon = P_t/\tau$, is used to depict the results obtained at each hop and then averaged over ten million iterations. It can be noticed that the simulation result are quiet close to the results of the proposed analytical model. Further notice that as the number of nodes, N, increases, the one-hop success probability also increases, indicating an

increased diversity gain. A small SNR margin is required by the system to achieve a certain probability of success as the number of N increases. For all the results, we assume identical values of σ and Rice K-factor, κ for signals from multiple transmitting nodes, along with path loss exponent, $\beta = 2$.

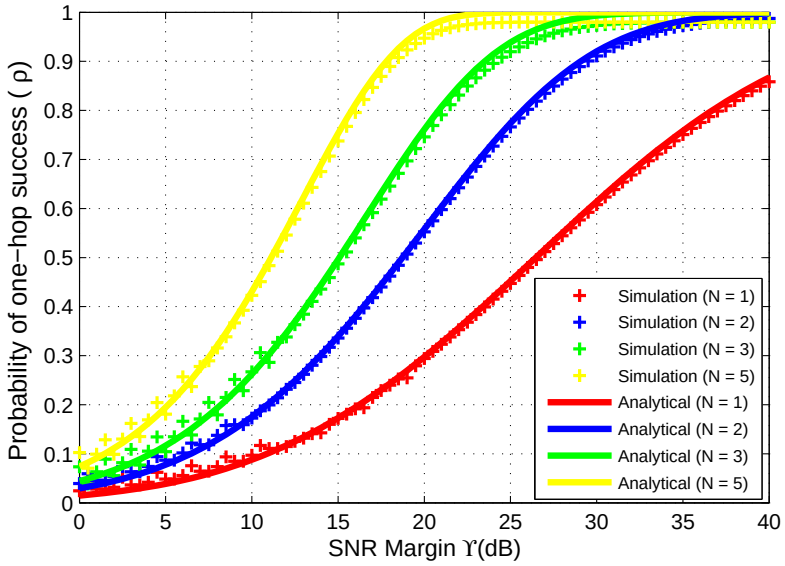

Figure 5.7: Simulation versus analytical results for $L = 5, \beta = 2, \sigma = 6dB$

In Fig. 5.8, the effect of shadowing in terms of σ is shown on the one-hop success probability, ρ. It can be noticed that at low SNR margins, an increase in σ increases the ρ. This is because, the variations in the received power across a certain mean is defined by σ, and the mean in turn is defined by the path loss exponent; the higher the variations, the higher the σ. This implies that at low SNR margin the system is path loss limited and as the signal propagates through the wireless medium, the path loss is dominant, thus, suppressing the effect of shadowing severity, and we might get a favourable response for an increase in σ, i.e, increase in one-hop success probability.

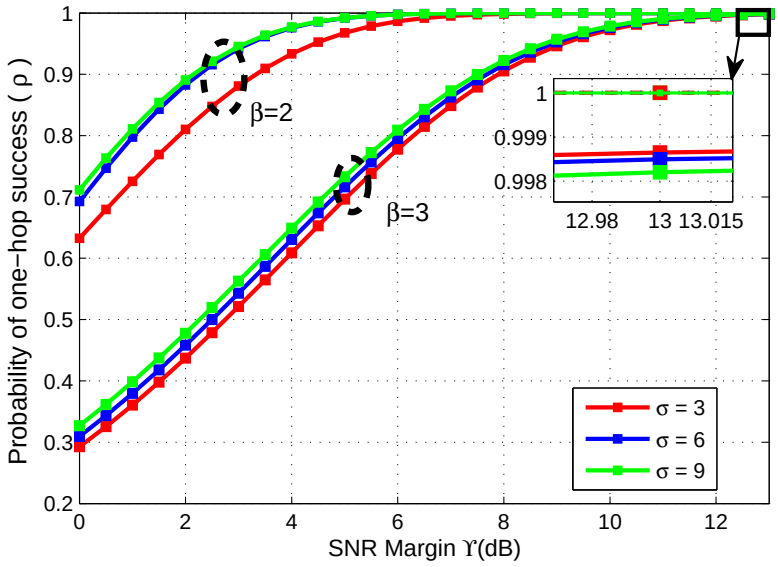

Figure 5.8: Varying standard deviation for different values of path loss exponent $N = 3, L = 2$

Whereas, path loss is compensated as the SNR margin increases and the shadowing severity starts to play its role. Hence, in Fig. 5.8 inset, reverse phenomena is depicted. As the SNR margin attains higher values, the path loss decreases and only the severity of shadowing causes the probability of success to drop for larger values of σ. Furthermore, from the same figure it can be noticed that as the path loss exponent, β, is increased, an overall degradation in the performance of the system can be observed.

The behavior of the path loss can also be attributed from Fig. 5.9, where an increase in length, L, of the region increases the average distance between two hops, whereas, number of nodes $N = 3$ remains fixed. This, results in larger signal attenuation and hence the probability of success drops.

In Fig. 5.10, the effect of Rice K-factor, κ, is observed by keeping $\sigma =$

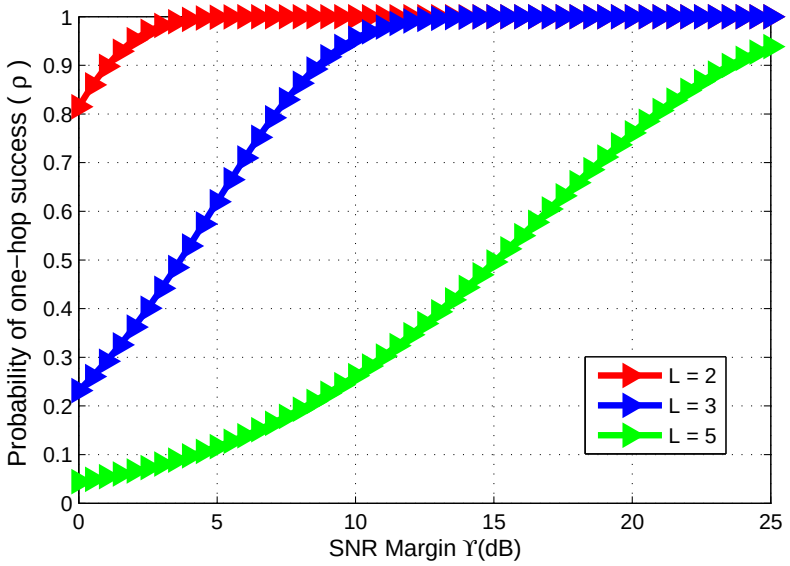

Figure 5.9: Success probability for different value of region length, $N = 3, \beta = 2$

$6dB$. We consider a fixed network size, $L = 2$, and a fixed number of nodes, $N = 3$, to observe the effect of κ. As the SNR margin attains higher values, the one-hop success probability increases as we increase the value of K-factor. It can be noticed that as much as $2dB$ of additional SNR margin is required if the environment becomes NLOS ($\kappa = 0$, Rayleigh fading) as compared to LOS when $\kappa = 10$. The deployment of a sensor network depends highly on the type of environment and the SNR margin should be adjusted accordingly for a desired quality of service (QoS).

The performance of the multi-hop strip networks depends on the probability of a message to successfully reach a certain destination without going into absorbing state. This end-to-end success probability is defined by QoS parameter, η, which is important to determine the coverage range of the network. For example, if we require to reach a certain distance with 80% QoS

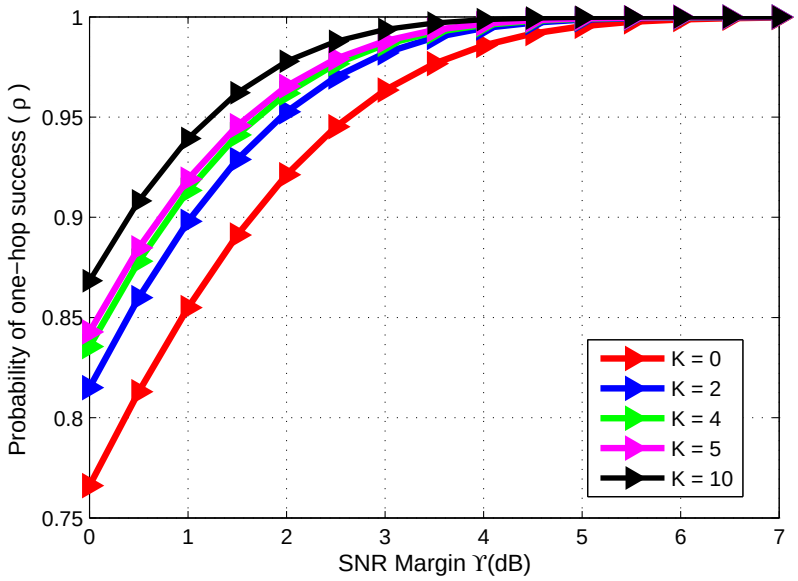

Figure 5.10: Success probability vs. SNR margin for varying K-factor

then $\eta = 0.8$. The message signal in our model can propagate a maximum of n-hops until the killing occurs, as shown in (4.4). For a fixed set of network parameters (path loss exponent, β, region length, L and transmit power, P_t) the ρ has a fixed value. Hence the QoS parameter sets an upper bound to the success probability of n-hop count, i.e., $\eta \leq \rho^n$. The maximum number of hops the message can travel is given by

$$n \leq \frac{\ln \eta}{\ln \rho} \tag{5.1}$$

To calculate the network coverage range, the product of n(obtained from (5.1)) and the length of the region, L, will provide the maximum distance a message can propagate while achieving a certain QoS. In Fig. 5.11, the coverage range contours against length of the region L and SNR margin, Υ, are illustrated for $\eta = 0.85$ and $N = 2$. The drop in maximum hop count as

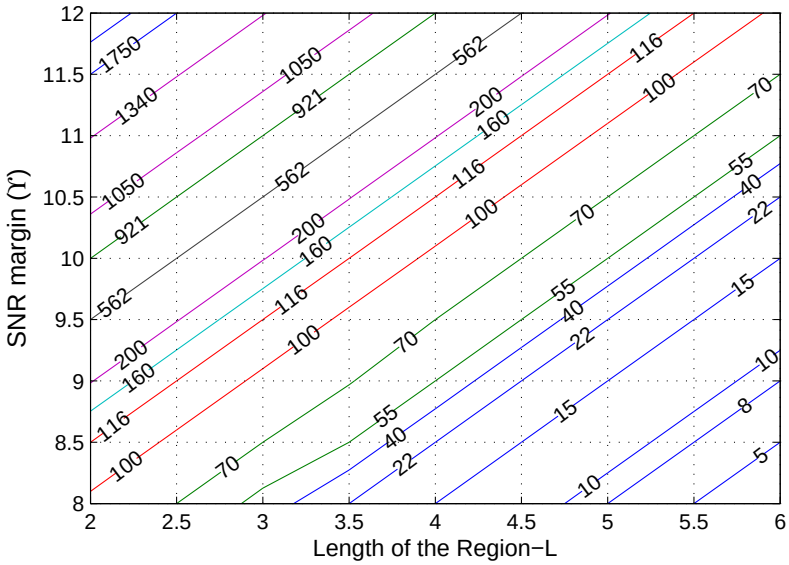

Figure 5.11: Coverage range for the extended strip network for $N = 2, \sigma = 6dB$ and $\eta = 0.85$

the value of L stretches depicts the distinct effect of path loss, as a fact that we are increasing the average distance between the hops. From this plot, a network designer can set various different combination of network parameters to attain certain value of network coverage. A network with latency constraint can achieve a given coverage range with fewer number of hops at the expense of high SNR margin (transmit power, P_t), whereas, networks with power constraint can achieve same coverage by reducing the hop size. For instance, if coverage range of 200 is desired, then former performance (delay-limited) can be achieved by using $L = 4.6$ and $\Upsilon = 11.5dB$. However, for the latter performance (energy-efficiency), $L = 2$ and $\Upsilon = 9dB$ can be used.

Chapter 6

Conclusion and Future Work

In this thesis, we have derived an analytical probability model for a 2-D network, where nodes cooperate with each other for transmission from one level to another, which is modeled as a quasi-stationary Markov chain. Corresponding to that, a transition matrix is derived by considering the channel as joint lognormal-Rice fading. An MGF-based technique along with Gauss-Hermite integration is used to find this joint distribution, where the sum of these lognormal-Rice RVs is approximated by a single lognormal RV. The effect on network's coverage area for some specific SNR margin required to achieve a certain QoS is quantified as a function of various parameters. For future this work can be extended for the 2-D random model, in which nodes are placed at random location.

Where in the later research work a strip-shaped extended network is studied by developing a discrete-time Markov chain model. We analysed the network under the impact of three random processes, i.e., lognormal shadowing, Rice fading and Weibull random distance. We derived the success probability of all nodes in adjacent regions using a three step process. First, we derived a

product distribution between inverse Weibull RV and lognormal RV and approximated it as another lognormal RV using a moment matching approach. The MGF-based method along with Gauss-Hermite integration is used to determine the product of resulting lognormal RV with Rice RV, where the sum of these lognormal-Rice RVs is approximated with a single lognormal RV. Corresponding to the Markov chain with quasi stationary distribution and the derived coverage probability, a transition matrix is derived using a simple binomial equation. A specific SNR margin is quantified for the network coverage range of the network as a function of different parameters. In future, the model can be studied by removing the hop boundary constraints and to analyse the network for random number of nodes at each level.

Bibliography

[1] B. R. Stojkoska, A. P. Avramova, and P. Chatzimisios, "Application of wireless sensor networks for indoor temperature regulation," *International Journal of Distributed Sensor Networks*, vol. 2014, Article ID 502419, 10 pages, May 2014.

[2] L. Zhang, D. Gao, C. H. Foh, D. Yang and S. Gao, "A survey of abnormal traffic information detection and transmission mechanisms," *International Journal of Distributed Sensor Networks*, vol. 2014, Article ID 582761, 13 pages, May 2014.

[3] L. Thanayankizil, A. Kailas, and M.A. Ingram, "Routing for wireless sensor networks with an Opportunistic Large Array (OLA) Physical Layer," *Ad Hoc and Sensor Wireless Networks, Special Issue on the 1st International Conference on Sensor Technologies and Applications*, vol. 8, no. 1-2, pp. 79-117, 2009.

[4] M. Hussain and S. A. Hassan, "Performance of multi-hop cooperative networks subject to timing synchronization errors," *IEEE Trans. Commun.*, vol. 63, no. 3, pp. 655-666, March 2015.

[5] A. Scaglione, Y.W. Hong, "Opportunistic large arrays: Cooperative transmission in wireless multi-hop ad hoc networks to reach far distances", *IEEE Trans. Signal Process.*, vol. 51, no. 8, pp. 2082–92, 2003.

[6] M. Hussain and S. A. Hassan, "The effects of multiple carrier frequency offsets on the performance of virtual MISO FSK systems", *IEEE Signal Process Letters*, vol. 22, no. 7, pp. 905-909, July 2015.

[7] Changcai Han and Si Li, "Distributed Testbed for Coded Cooperation with Software-Defined Radios," *International Journal of Distributed Sensor Networks*, vol. 2013, Article ID 325301, 9 pages, 2013. doi:10.1155/2013/325301

[8] S. H. Kabir, M. S. Omar, S. A. Raza, M. Hussain, S. A. Hassan, "Demonstration and implementation of energy efficiency in cooperative networks", in *IEEE International Wireless Communications and Mobile Computing Conference (IWCMC)*, Croatia, Aug. 2015.

[9] M. S. Omar, S. A. Raza, S. H. Kabir, M. Hussain, S. A. Hassan, "Experimental implementation of cooperative transmission range extension in indoor environments", in *IEEE International Wireless Communications and Mobile Computing Conference (IWCMC)*, Croatia, Aug. 2015.

[10] M. Bacha and S. A. Hassan, "Distributed versus cluster-based cooperative linear networks: A range extension study in Suzuki fading environments," *Proc. IEEE Personal Indoor and Mobile Radio Communications (PIMRC)*, London, UK, Sept. 2013.

[11] S. A. Hassan, "Range extension using optimal node deployment in linear multi-hop cooperative networks," *IEEE Radio and Wireless Symposium (RWS)*, Austin, Texas, Jan. 2013.

[12] S. A. Hassan and M. A. Ingram, "The benefit of co-locating groups of nodes in cooperative line networks," *IEEE Commun. Letters*, vol. 16, no. 2, pp. 234-237, Feb. 2012.

[13] S. A. Hassan and M.A. Ingram, "On the modeling of randomized distributed cooperation for linear multi-hop networks," *IEEE Intl. Conf. Communications (ICC)*, Ottawa, Canada, June 2012.

[14] S. A. Hassan, "Performance analysis of cooperative Multi-hop strip networks," *Springer Wireless Personal Communications*, vol. 74, no. 2, pp. 391-400, Jan. 2014.

[15] S. A. Hassan and M. A. Ingram, "Analysis of an Opportunistic Large Array line network with bernoulli node deployment", *IET Communications*, vol. 8, no. 1, pp. 19-26, Jan. 2014.

[16] M. Bacha and S. A. Hassan, "Performance analysis of cooperative linear networks subject to composite shadowing fading," *IEEE Trans. Wireless Commun.*, vol. 12, no. 11, pp. 5850-5858, Nov. 2013.

[17] M. Bacha and S. A. Hassan, "Coverage aspects of cooperative multi-hop line networks in correlated shadowed environment", *IEEE International Conference on Computing, Networking and Communications (ICNC)*, Hawaii, United States, Feb. 2014.

[18] S. Wyne, A. P. Singh, F. Tufvesson, and A. F. Molisch, "A statistical model for indoor office wireless sensor channels," *IEEE Trans. Wireless Commun.*, vol. 8, no. 8, pp. 4154–4164, Aug. 2009.

[19] B. S. Mergen and A. Scaglione, "A continuum approach to dense wireless networks with cooperation," in *Proc. 2005 IEEE INFOCOM*, pp. 2755–2763.

[20] S. A. Hassan and M. A. Ingram, "A quasi-stationary Markov chain model of a cooperative multi-hop linear network," *IEEE Trans. Wireless Commun.*, vol. 10, no. 7, pp. 2306–2315, July 2011.

[21] R. I. Ansari and S. A. Hassan, "Opportunistic Large Array with limited participation: An energy-efficient cooperative multi-hop network", *IEEE International Conference on Computing, Networking and Communications (ICNC)*, Hawaii, United States, Feb. 2014.

[22] Y. J. Chang, H. Jung, and M. A. Ingram, "Demonstration of an OLA-based cooperative routing protocol in an indoor environment," *in Proc. 17th Eur. Wireless Conf.*, pp. 1–8, April 2011.

[23] L. V. Thanayankizil, A. Kailas, and M. A. Ingram, "Opportunistic Large Array Concentric Routing Algorithm (OLACRA) for upstream routing in wireless sensor networks," *Ad Hoc Networks*, vol. 9, pp. 1140–1153, Sept. 2011.

[24] C. Capar, D. Goeckel, D. Towsley,"Broadcast analysis for large cooperative wireless networks,' *arXiv preprint arXiv*:1104.3209, 2011

[25] T. R. Halfold and K. M. Chugg, "Barrage relay networks," *in Information Theory and Applications Workshop*, Feb. 2010.

[26] A. Kailas and M. A. Ingram, "Alternating opportunistic large arrays in broadcasting for network lifetime extension," *IEEE Trans. Wireless Commun.*, vol. 8, no. 6, pp. 2831-2835, June 2009.

[27] A. Afzal and S. A. Hassan, "Stochastic modeling of cooperative multihop strip networks with fixed hop boundaries", *IEEE Trans. on Wireless Commun.*, vol. 13, no.8, pp. 4146-4155, Aug. 2014.

[28] A. Afzal and S. A. Hassan, "A stochastic geometry approach for outage analysis of ad hoc SISO networks in Rayleigh fading", *IEEE Global Communication Conference (Globecom)*, Atlanta, Georgia, Dec. 2013.

[29] S. Wyne, A. P. Singh, F. Tufvesson, and A. F. Molisch, "A statistical model for indoor office wireless sensor channels," *IEEE Trans. Wireless Commun.*, vol. 8, no. 8, pp. 4154–4164, Aug. 2009.

[30] S. S. Syed and S. A. Hassan, "On the use of space-time block codes for Opportunistic Large Array Network," *IEEE International Wireless Communications and Mobile Computing Conference (IWCMC)*, Nicosia, Cyprus, Aug. 2014.

[31] N. B. Mehta, J. Wu, A. F. Molisch, and J. Zhang, "Approximating a sum of random variables with Lognormal," *IEEE Trans. Wireless Commun.*, vol. 6, no. 7, July 2007.

[32] V. Naghshin, A. M. Rabiei, N. C. Beaulieu, M. C. Reed, B. Maham, "Interference analysis for square-shaped wireless networks with uniformly

distributed nodes," *IEEE Global Communications Conference (GLOBECOM)*, pp. 217-221, Dec. 2014.

[33] Y.J. Chang and M.A. Ingram, "Cluster transmission time synchronization for cooperative transmission using software defined radio," in *IEEE (ICC) Workshop on Cooperative and Cognitive Mobile Networks (CoCoNet3)*, May 2010.

[34] C.D. Meyer, *Matrix Analysis and Applied Linear Algebra*, SIAM publishers, 2001.

[35] G. L. Stuber, *Principles of Mobile Communications*, 3rd ed. Springer Publisher, 2011.

[36] M. Abramowitz and I. Stegun, *Handbook of Mathematical Functions with Formulas, Graphs, and Mathematical Tables*, 9th ed. Dover, 1972.